Journal of Cell Science 106, 377-387 (1993)
Printed in Great Britain © The Company of Biologists Limited 1993

Adhesion of CHO cells to fibronectin is mediated by functionally and structurally distinct adhesion plaques

Léone Tranqui[1,*], Yves Usson[2], Christiane Marie[1] and Marc R. Block[1,†]

[1]Laboratoire d'Etude des Systèmes Adhesifs Cellulaires, A.T.I.P.E. de l'URA 1178 du CNRS and [2]Laboratoire RFMQ-TIM3 USR B00690 du CNRS, Université Joseph Fourier, BP 53X, F38041 Grenoble Cedex, France

*Present address: Centre de Physiologie et de Physiopathologie, Université J. Fourier, BP 53X, F38041 Grenoble Cedex, France
†Author for correspondence

SUMMARY

We have investigated the dynamics between free fibronectin receptors and clusters of them organized into adhesion plaques on CHO cells using the ability of these free integrins to be endocytosed and recycled to the plasma membrane. Indirect inhibition of the endocytic cycle by monensin resulted in the subsequent internalization of free receptors, which we followed by indirect immunostaining and confocal microscopy. Consequently, all the adhesive structures that were in equilibrium with free integrins became progessively disorganized. The cellular morphological changes were analyzed and correlated with the distribution of cell-substratum contacts viewed by confocal images obtained after immunostaining with antibodies raised against the fibronectin receptor, talin, vinculin and actin. After cell adhesion to fibronectin, blockage of the endocytic cycle induced disruption of the adhesion plaques that were mainly localized at the cell periphery, and disappearance of the stress fibers. However, the cells remained firmly attached to the substratum through focal contacts localized in the central part of the cell. These central focal contacts, but not the peripheral adhesion plaques, could form when the vesicular traffic was blocked prior to adhesion and they allowed the cells to attach and flatten onto the substratum. Whereas both adhesive structures contained the same receptors linked to talin and vinculin, the central adhesive structures were attached to a short stretch of actin but never permitted the organization of stress fibers.

Key words: adhesion plaques, fibronectin, integrin, talin, endocytosis

INTRODUCTION

We suggest that adhesion of CHO cells is mediated by two types of adhesion plaques. The cells attach and flatten using receptors that cluster to form central focal contacts; but complete spreading is achieved by dynamic peripheral adhesion plaques in equilibrium with a pool of free fibronectin receptors that are subjected to the endocytic cycle.

CHO cells can attach to fibronectin, a component of the extracellular matrix, using a specific receptor (Brown and Juliano, 1985). This membrane glycoprotein is a member of the integrin superfamily (for review see Hynes, 1992; Ruoslahti, 1991; Dedhar, 1990). The fibronectin receptor (FnR) of CHO cells is the counterpart of the human VLA_5 (Hemler, 1990). Upon adhesion, the FnRs cluster into highly organized cellular structures named adhesion plaques or focal contacts that link the extracellular matrix to actin microfilaments and a number of cytoskeleton proteins such as talin, vinculin and α-actinin (for review see Turner and Burridge, 1991).

On CHO cells in suspension, FnRs are constitutively internalized (Sczekan & Juliano, 1990). Recycling occurs to the plasma membrane from an intracellular pool (Bretscher, 1989). However, heterogeneous populations of FnR have been described on CHO cells, one of which (70-75% of total receptors) might be unavailable for rapid internalization and recycling (Sczekan and Juliano, 1990). This heterogeneity may reflect some specialized functions of the FnRs, with respect to cell adhesion. Since it has been shown that immobile spread-out cells exhibit reduced lateral mobility of their integrins at focal contacts (Duband et al., 1988), it was assumed that these latter structures are mainly static. However, the question of whether turnover of the integrins could take place within adhesion plaques through the endocytic cycle has never been investigated and remains open.

To address this question, an ionophore such as monensin (Basu et al., 1981; Berg et al., 1983; Harford et al., 1983a,b) or a weak base such as chloroquine (Gonzalez-Noriega et al., 1980; Van Leuven et al., 1980; Maxfield, 1982) can be used. These drugs block the recycling of the internalized receptors but do not prevent endocytosis. Therefore, if the integrins located at focal contacts were exchanged with free

receptors that are subjected to the endocytic cycle, the progressive loss of surface receptor induced by monensin or chloroquine should disorganize the adhesive structures. Conversely, if the integrins involved in adhesion plaques were not exchanged with free receptors, or if these receptors were unavailable to the endocytic cycle, these structures should be resistant to the action of the drugs.

In this paper, we have analyzed the cellular morphological changes induced by monensin or chloroquine in correlation with the distribution of the adhesive structures viewed by confocal images obtained after immunostaining with antibodies raised against FnR, talin, vinculin or actin. We report that the use of ionophores has allowed us to distinguish between two types of contacts: thick peripheral adhesion plaques, which disappeared during monensin incubation at 37°C, and thinner central adhesion plaques, which were resistant to the drugs. Our data suggest that in peripheral adhesion plaques fibronectin receptors are exchanged with free receptors that are subsequently internalized and recycled, whereas in central focal contacts, either this exchange does not occur or the integrins are unavailable for endocytosis.

MATERIALS AND METHODS

Protein purification

Human fibronectin was purified by affinity chromatography according to the method of Engvall and Ruoslahti (1977). Human talin was extracted from outdated platelets from the Blood Center of Grenoble and purified as previously described (Turner and Burridge, 1988).

Cell culture

Wild-type CHOwere grown either on plates or in spinners in Minimum Essential Medium with alpha modification (α-MEM), supplemented with 7.5% foetal calf serum. They were harvested with Hanks' Balanced Salt Solution (HBSS) supplemented with 1 mM EDTA and 0.05% trypsin (w/v).

Antibodies

Monoclonal antibodies against vinculin (clone V284) were obtained from Boehringer Mannheim Biochemica. Human anti-actin was a gift from Dr Micouin, from the Blood Center of Grenoble, this antibody raised against human actin and coupled to agarose beads retains a high specificity to actin. Monoclonal antibody against FnR (clone PB1) was a generous gift from Dr Juliano, from Chapel Hill University, North Carolina. The monoclonal antibody against the 190 proteolytic fragment of human talin (clone 1B10), was raised in our laboratory. IgG1 was purified from ascitic fluid by 50% ammonium sulfate precipitation. The pellet was resolubilized in a 3.3 M NaCl, 100 mM borate buffer, pH 8.9, and dialyzed against it overnight. High-pressure affinity chromatography of IgG1 was carried out using a 5 ml Protein A-Trisacryl column (Merck) washed successively with 3 M NaCl, 50 mM borate, pH 8.9, and 3 M NaCl, 10 mM borate, pH 8.9, and eluted with 100 mM glycine at pH 3 at a flow rate of 0.2 ml/min. The eluted fractions were immediately neutralized with a few drops of 1 M Tris-HCl, pH 8. The purified antibody efficiently recognizes the purified human and chicken talin and the p190 fragment in solid-phase assays. It gives a specific immunofluorescence staining of the adhesion plaques that can be completely displaced by large concentrations of pure talin.

Monensin- or chloroquine-treated cells

Monensin and chloroquine were from Sigma. Depending on the experiment, cells were seeded either on 35 mm Petri dishes (Falcon, Labware), or on glass coverslips placed in 35 mm Petri dishes. In all the experiments described here cells were grown on a fibronectin coat deposited as already described (Tranqui et al., 1992). Drugs were added to the cells before or after adhesion.

For studying drug action before cell adhesion, 1.0 ml of a cell suspension (1×10^5 cells/ml) in α-MEM medium containing 20 mM HEPES, pH 7.0, and 25 μM monensin or 10 μM chloroquine, was poured into a 35 mm Petri dish and allowed to adhere for 4 h.

For studying drug action on spread-out cells, the suspension was plated onto dishes in HEPES/α-MEM medium for 4 h at 37°C. Then the medium was removed from the adherent cells and replaced with the same medium supplemented with 25 μM monensin, and the incubation was followed for an other period of 4 h at 37°C or 4°C.

Control experiments were carried out under the same conditions but drugs were omitted.

Morphometric analysis

Samples prepared as decribed above were rinsed three times with HBSS, then they were immersed in 3% paraformaldehyde in PBS at 37°C for 10 min. Permeabilization was achieved by incubation in 1% Triton X-100 in PBS, for 15 min. The contrast was improved with trypan blue staining. The slides were analyzed by means of a SAMBA 2005 image cytometer (Alcatel TITN, Grenoble France) connected to a Zeiss microscope (objective ×40, 1.3 NA, oil). Four different regions selected systematically from the top to the bottom of the slides were analyzed. The average number of cells measured per slide was 300. The elongation factor (Russ, 1990), the projection area and the form factor were determined for each cell with a cytometer. The elongation factor is equal to the ratio between the maximum diameter and the minimum diameter of the cytoplasm. The form factor is equal to the ratio of the square perimeter to the projection area weighted by 4π. These variables translate how far a shape diverges from a perfect circle. The form factor is equal to unity for a perfect circle and increases when the shape becomes elliptical or when the cell contour becomes more and more complicated.

Cell adhesion assays

To test the inhibition of adhesion by an anti-FnR antibody, cells seeded on 35 mm Petri dishes for 4 h with or without monensin (as described above), were incubated with 10 or 1 μg/ml of PB1 at 37°C. At low PB1 concentrations the dishes were gently washed and the remaining adherent cells were photographed under phase contrast, and counted. The number of adherent cells in a constant unit area (0.03 mm^2) was estimated. All adhesion assays were run in triplicate, and for each sample 2 areas were counted. Results were compared with controls without monensin and PB1 (100% of adhesion).

Immunofluorescence studies

Fibronectin receptors, talin, vinculin and actin, were detected by indirect immunofluorescence on cells grown on coated glass coverslips. Samples treated with or without monensin or with low concentration of PB1 were analyzed. We used the modified method of Granger and Lazarides (1979). Briefly, cells were washed three times with PBS at 37°C and then immersed in freshly made 3% paraformaldehyde in PBS at 37°C for 10 min. Permeability to antibodies was achieved with incubation in 1% NP40 in PBS, for 30 min. After a 5 min wash in PBS, the antibody solution was added to the preparation and incubated for 30 min at

37°C. Fluorescent labeling was achieved with a 30 min incubation with a rhodamine-conjugated $F(ab')_2$ solution at 37°C. Finally, the cells were washed for 15 min in PBS and water, and mounted in a mixture made of Mowiol and glycerol in which 1,4-diazobicyclo-(2.2.2)-octane (DABCO) was added. Observations were carried out either with a Zeiss confocal microscope, or with a Nikon microphot microscope equipped for epifluorescence.

Microscopy

The morphology of living CHO cells treated with monensin or choroquine, or untreated samples, was observed by phase-contrast microscopy with an inverted light microscope (Diaphot Nikon) equipped with a Ph2 plan 20, NA 0.5 objective lens.

Interference reflection microscopy (IRM) was performed with a Nikon microphot FxA microscope equipped with a polarizer, an analyser oriented at 90° to the polarizer, and a NPL Fluotar ×50 oil immersion, NA 1.00 objective lens (Leitz) equipped with a rotatable quarter wavelength quartz plate mounted on the front lens. The preparations were epi-illuminated at 546 nm using and interference filter (10 nm band pass) located in front of the polarizer.

Confocal microscopy was performed by the indirect immunofluorescence technique using anti-talin, anti-vinculin or anti-actin antibodies, and the confocal imaging system (model LSM10 ZEISS, Oberkochen) equipped with a Planapo ×63 oil immersion, NA 1.40 objective lens. An argon laser (λ = 514 nm) was used to excite the dye, and the emission signal above 590 nm was collected. The micrographs represent an optical section 0.2 μm thick. Imaging improvements were obtained using a similar system to AVEC enhancement techniques. Briefly, the signal-to-noise ratio was improved when 16 frames were accumulated to form an image (Allen et al., 1981).

RESULTS

Monensin or chloroquine induce morphological changes in adhesive CHO cells

Wild-type CHO cells were suspended in α-MEM/HEPES and seeded without monensin on fibronectin-coated Petri dishes. They were allowed to attach and spread onto the substratum, then monensin was added and further incubation was carried out for 4 h as described under Materials and Methods. Alternatively, monensin was added prior to cell spreading, and the incubation was carried out for 4 h at 37°C. Compared to the polygonal shape of control cells (Fig. 1A), monensin treatment of spread-out cells induced a significant morphological change as viewed by phase-contrast microscopy (Fig. 1B): the cells rounded up but did not separate from the fibronectin coat and remained flat. On the other hand, when monensin was added prior to cell spreading, it did not hamper the cell attachment to and initial spreading phase onto fibronectin. Typical round but flat cells were observed (Fig. 1C). Thus, the final step of spreading resulting in polygonal cells was never reached.

The modifications of cell shape were quantified and analyzed on the basis of the elongation factor (major axis/minor axis) measurements on a statistically significant number of samples (300 cells) (Table 1). Clearly, the modifications observed were significant (Student's *t*-test $P<0.005$). Furthermore, adding monensin before or after spreading resulted in a very similar final shape of the cell, significantly distinct from those of the untreated control cells. This

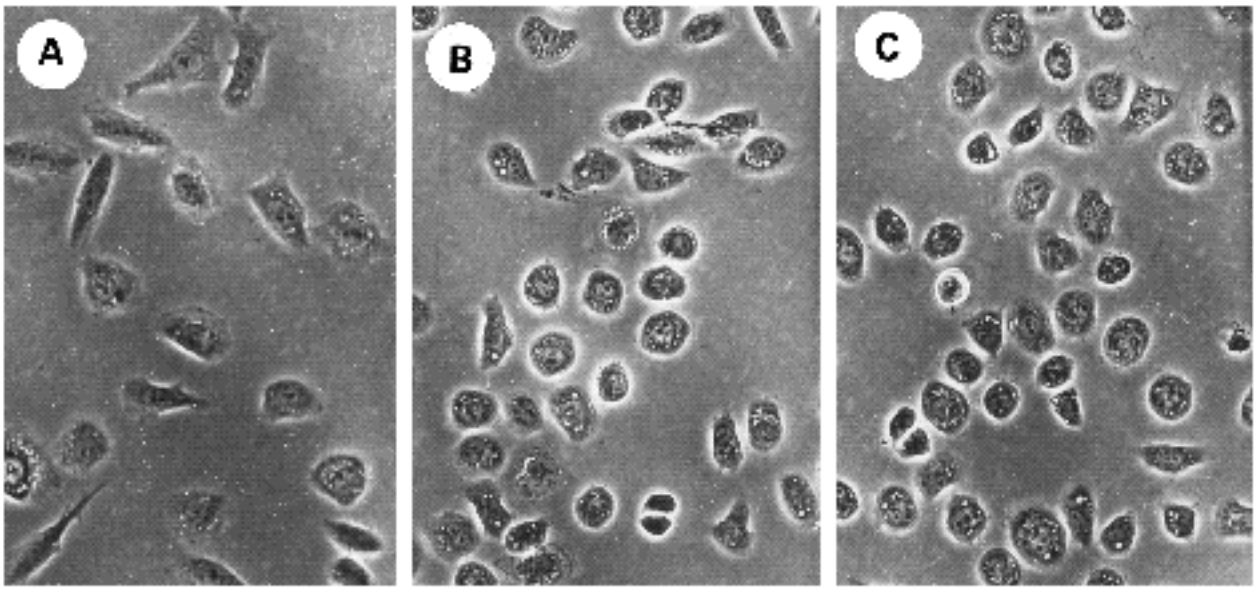

Fig. 1. Morphology of control and monensin-treated CHO cells grown on fibronectin-coated Petri dishes. Wild-type CHO cells in α-MEM supplemented with 7.5% foetal calf serum (FCS) are grown in a monolayer and subsequently treated with 0.05% trypsin and 1 mM EDTA in Hanks' Balanced Salt Solution (HBSS). After washing in HBSS, the cells are resuspended in α-MEM supplemented with 20 mM HEPES at pH 7 without FCS. The cells are seeded on fibronectin-coated Petri dishes at a concentration of 1×10^5 cells/ml and incubated at 37°C in different experimental conditions. (A) Untreated CHO cells after 4 h at 37°C. (B) After a preincubation time of 4 h at 37°C, monensin is added at a final concentration of 25 μM and the incubation is continued for 4 h. (C) CHO cells are seeded in α-MEM supplemented with 25 μM monensin and allowed to attach and spread on fibronectin at 37°C for 4 h. The phase-contrast pictures were obtained at a magnification of ×200 using a Diaphot Nikon inverted microscope equipped with a Ph2 plan 20, NA 0.50 objective lens.

Table 1. Elongation factors of spread-out CHO cells treated with ionophores

Spreading conditions	Post-spreading treatment	Elongation factor (major axis/minor axis)
4 h, 37°C	4 h, 37°C	1.60±0.38
4 h, 37°C	None	1.60±0.44
4 h, 37°C	4 h, 4°C	1.60±0.46
4 h, 37°C + monensin	None	1.43±0.32
4 h, 37°C	4 h, 37°C + monensin	1.45±0.19
4 h, 37°C	4 h, 4°C + monensin	1.63±0.45
4 h 37°C + chloroquine	None	1.45±0.26

For each sample, the average number of cells analyzed was 300, selected from four different regions of the slide.

morphological change was not observed when monensin was added to fully spread-out cells at 4°C, Similarly, addition of choloroquine before spreading reduced the elongation factor of the cells to 1.45 ± 0.26, a value close to those obtained with monensin, whereas this permeable amine was less efficient than the ionophore when it was added after spreading. Since both drugs inhibit the endocytic cycle by distinct mechanisms, these results suggest that the morphological changes observed might be related to the endocytosis and recycling of some FnRs. This interpretation was further supported by the absence of any observed effect when monensin was added to the spread out cells at 4°C, a temperature that blocks endocytosis and cellular traffic.

Furthermore, the intracellular pattern of FnR distribution, viewed in a confocal section located at 1.8 μm from the fibronectin-coated glass (i.e. above the adhesion plaques), showed very weak immunostaining with the monoclonal antibody PB1 in control cells (Fig. 2C). This result was consistent with the low level of the intracellular FnRs that represents only 15% of the total number (Bretscher, 1989). Conversely, upon monensin treatment, a dramatic increase in the concentration of the intracellular receptors was detected (Fig. 2D). Since both experiments were performed in the presence of 10 μg/ml of cycloheximide to prevent

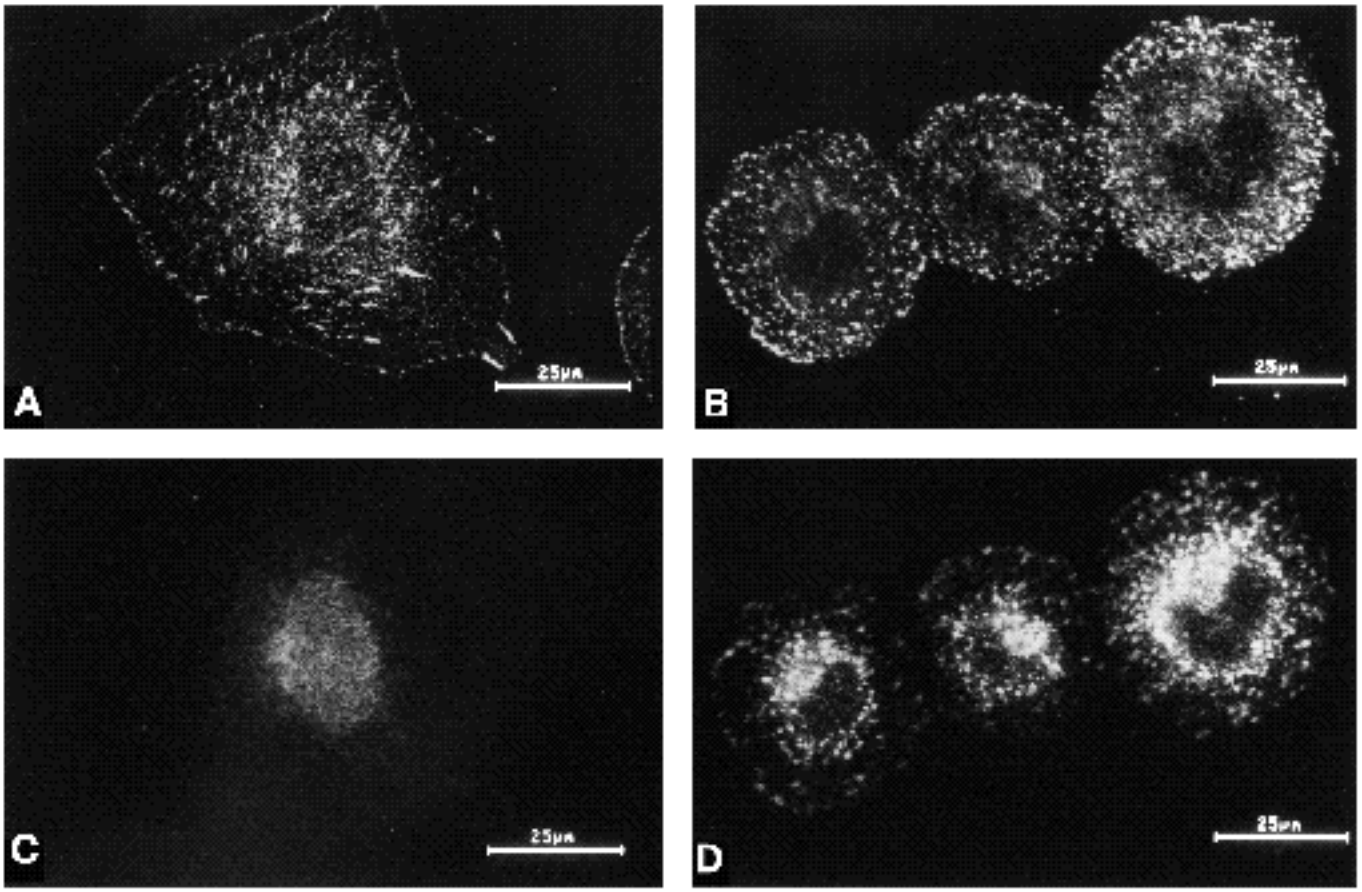

Fig. 2. Visualization of the internalization of FnRs upon monensin treatment of CHO cells. Indirect immunofluorescence staining was used to localize FnRs in basal and intracellular confocal sections. Cycloheximide-treated cells (10 μM) plated on fibronectin-coated coverslips were incubated with monensin (25 μM) as described under Materials and Methods. After 4 h, the cells were fixed with 3% paraformaldehyde and permeabilized according to the procedure described under Materials and Methods. Staining was performed with PB1, a monoclonal antibody raised against the hamster FnRs and an anti-mouse IgG $(Fab')_2$ coupled with rhodamine. Optical sections of 0.2 μm located at 0.66 and 1.8 μm from the fibronectin coat were analyzed. (A and C) Control cell. (B and D) Monensin-treated cells. (A and B) Optical sections located at 0.66 μm from the fibronectin coat where the best detection of the adhesion plaques is obtained. (C and D) Intracellular optical sections located at 1.8 μm from the fibronectin coat.

the synthesis of new proteins, the increase in the intracellular concentration of integrin was mainly due to the internalization of surface-located receptors, suggesting that receptors initially located in specific adhesion plaques were now present in the intracellular space. In the same experiments, optical sections located next to the fibronectin coat (0.66 μm) showed a punctate staining, suggesting the organization of adhesion plaques (Fig. 2A and B). However, in these optical sections the distribution of FnRs between adhesive structures was modified by monensin: in control cells (Fig. 2A) FnR clusters were mainly located at the center and on the periphery of the cells, whereas in monensin-treated samples the FnR clusters were smaller and their distribution was homogeneous, with no staining at the edges of the cells (Fig. 2B).

Monensin blocks the spreading but not the attachment of the cells

The kinetics of cell attachment and spreading were analyzed by means of the quantitative morphometric analysis of the cultured cells using a SAMBA 2005 image cytometer as described under Materials and Methods. For each cell, three measurements were made: the projection area of the cell, the perimeter of the cell, and the form factor. This analysis revealed that the initial phase of cell attachment was identical, with or without monensin present in the medium. In control experiments, this initial step of attachment and flattening of the cells was followed by a second phase of spreading that corresponded to an increase of the projected cell area and the form factor (Fig. 3). After one hour at 37°C, a plateau was reached, indicating the state of maximum spreading of the cells. However, when the ionophore was present, the spreading phase was not observed (Fig. 3), suggesting that either externalization of FnRs or high intracellular concentrations of potassium were required for cell spreading.

Monensin modifies the distribution of the cellular adhesive structures

The loss of the polygonal shape of the CHO cells induced by monensin or chloroquine suggested that the adhesion plaques located at the cell periphery were disorganized and subsequently disrupted. However, since the adhesion of the central part of the cells remained, it was likely that the central cellular adhesion sites were less affected by the drugs and allowed the cells to keep a flat architecture. In fact, the FnR, vinculin or talin clusters were smaller in monensin-treated cells (Fig. 2B, Fig. 4B and D), suggesting that these structures were also disorganized by the drug, but with slower kinetics. This hypothesis was confirmed by experiments using overnight incubation with monensin. Long-time exposure to the drug resulted in complete detachment of the CHO cells (not shown).

To determine whether the morphological change observed reflected a reorganization of the cellular adhesion sites, we analyzed the matrix-cell contacts viewed by indirect immunostaining using monoclonal antibodies raised against FnR, talin and vinculin, and in the confocal optical section 0.2 μm thick that was closest to the support (0.660 μm). In this section we observed a typical pattern of peripheral and central staining in control cells (Fig. 2A, Fig. 4A and C) using specific stainings for receptors, talin or vinculin. Since talin and vinculin were cytosolic proteins mainly located at adhesive structures, the pattern observed in Fig. 4 ruled out the hypothesis that the central staining observed with anti-FnR antibody might reflect endocytic vesicles located at the dorsal face of the membrane. This heterogeneity of staining with anti-FnR, anti-talin or anti-vinculin was never encountered in monensin-treated cells (Fig. 2B, Fig 4B and C).

The staining patterns that we obtained, which were specific to proteins located at adhesion plaques, suggested that we could distinguish between two types of focal contacts: typical adhesion plaques located at the edges of spread-out cells and central focal contacts. Whereas the former were sensitive to monensin, the latter were more resistant to the drug. IRM studies of control and monensin-treated cells (Fig. 5) indicated that the monensin-treated cells still exhibited faint but distinct dark areas that roughly correlated with the immunofluorescence staining using anti-vinculin monoclonal antibodies (Fig. 5C and D). This indicated that the immunostaining pattern represented true sites of adhesion to the fibronectin coat. On the other hand, IRM showed that monensin disrupted the pseudopodia of the

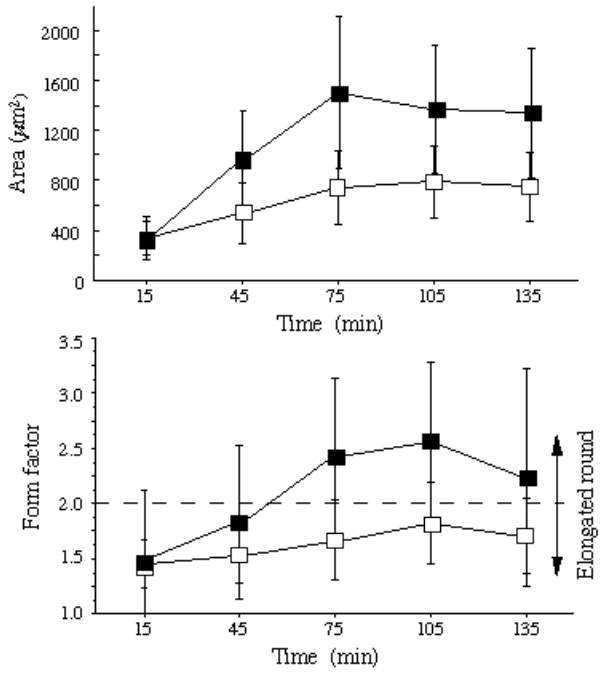

Fig. 3. Kinetics of cell attachment and spreading of control and monensin-treated CHO cells. After different incubation times (ranging from 15 min to 135 min) at 37°C in α-MEM supplemented with 20 mM HEPES, the adherent CHO cells were fixed with 3% paraformadehyde and permeabilized with 1% Triton X-100 in PBS. The permeabilized cells were stained with trypan blue and a morphometric analysis was performed as described under Materials and Methods on 300 cells for each experimental condition. The average projected cell area and form factor were estimated. Control and monensin-treated cells were analyzed in two parallel experiments. Filled rectangles represent kinetics performed with control cells. Open rectangles represent kinetics performed with monensin-treated cells.

cells, in good agreement with the dynamic nature of ruffling edges of the cells and the recycling of integrin receptors (Bretcher, 1989, 1992).

It is noteworthy that with control cells grown for 24 h in α-MEM supplemented with 7.5% foetal calf serum, a different distribution of the adhesive structures (viewed by the anti-vinculin immuno-staining) was observed (Fig. 6). Larger peripheral adhesion plaques were detected whereas no central focal contacts remained. A possible explanation for this reorganization might be that the serum has provided large amounts of other matrix components such as vitronectin, and has allowed the organization of heterogeneous clusters of distinct integrins. Such clusters might induced a different organization of the underlying cytoskeleton (Dejana et al., 1988; Charo et al., 1990). On the other hand, such a distribution of focal contacts may also occur following the initial phase of spreading. The cells grown for 24 h in medium supplemented with 7.5% foetal calf serum exhibited exhibited a stronger sensitivity to monensin, which resulted in a more dramatic morphological change (Fig. 7) after 4 h of incubations with the ionophore. This was consistant with the reduced number of central contacts that can be observed in Fig. 6 and with the dynamic nature of peripheral adhesion plaques.

Peripheral and central adhesion plaques have distinct organizations and properties

Analysis of consecutive confocal sections of untreated CHO cells stained with anti-talin, anti-vinculin or anti-actin and reconstitution of the images of transverse cuts indicated that central focal contacts and peripheral adhesion plaques have a different thicknesses. Conversely, with monensin-treated cells, the thinner adhesive structures were the only ones encountered (Table 2). This again pointed out that, a 4 h incubation with monensin at 37°C disorganized adhesion plaques located at the edges of the cells, but preserved those with a more central position.

These differences suggested either that a different organization of the clustering of the underlying FnRs was involved in the central focal contacts as compared to peripheral adhesion plaques, or that these receptors were different. However, the same types of FnRs should be involved in both structures, since the addition of 5 to 10 μg/ml of PB1, an anti-FnR monoclonal antibody that prevents cell adhesion on fibronectin(Brown and Juliano, 1985), induced complete detachment of the spread-out cells from the fibronectin coat. However, when tested, the addition of the PB1 antibody at a concentration of 1 μg/ml resulted in a striking variety of cell shapes with very few focal contacts at the central core, whereas some peripheral pads at the

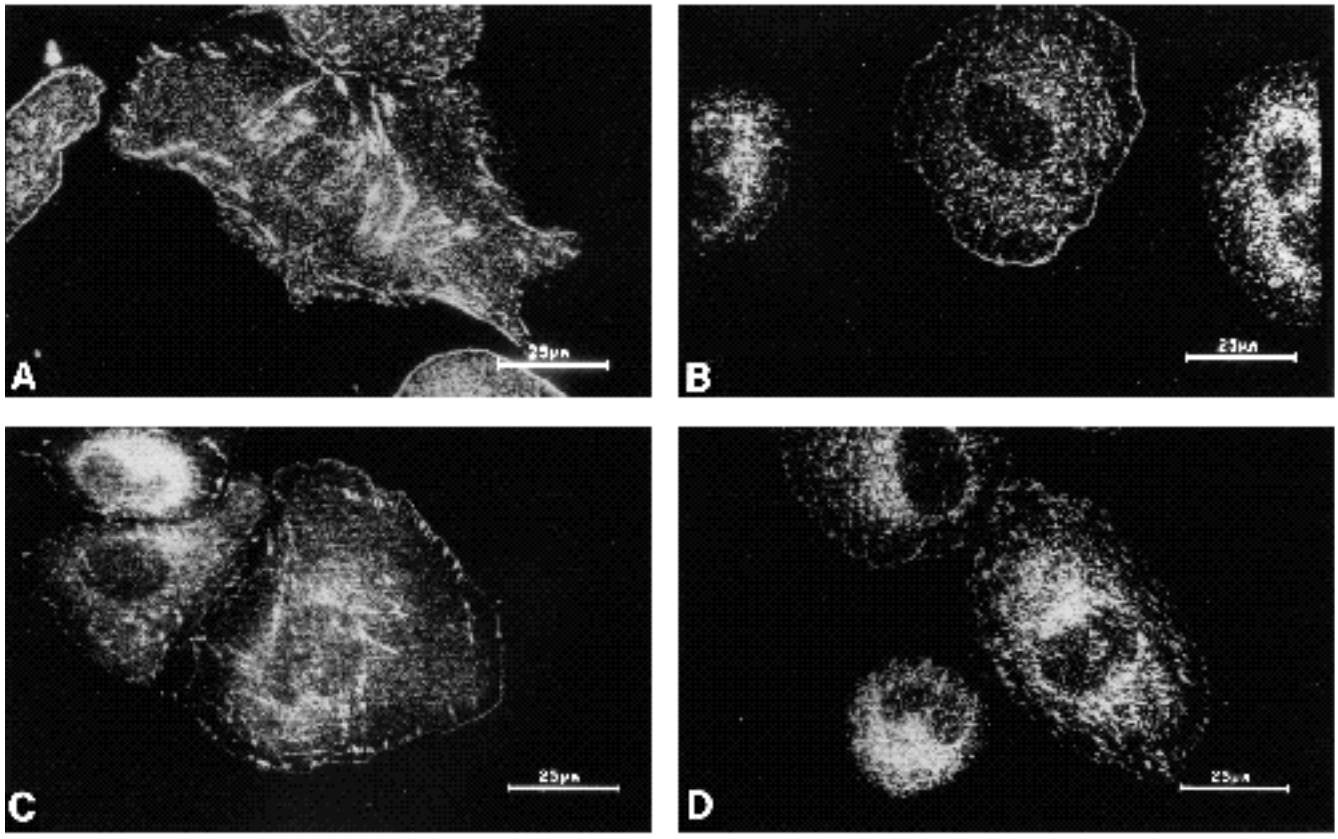

Fig. 4. Immunofluorescence staining of adhesion plaques with anti-talin and anti-vinculin monoclonal antibodies in control and monensin-treated CHO cells. The cells were seeded onto fibronectin-coated glass coverslips and allowed to attach and spread for 4 h at 37°C. Microscopy was carried out as described under Materials and Methods. (A and B) Immunofluorescence staining using anti-talin antibodies (clone 1B10). (C and D) Immunofluorescence staining using anti-vinculin antibodies. (A and C) Control cells. (B and D) Monensin-treated cells. Bars, 25 μm.

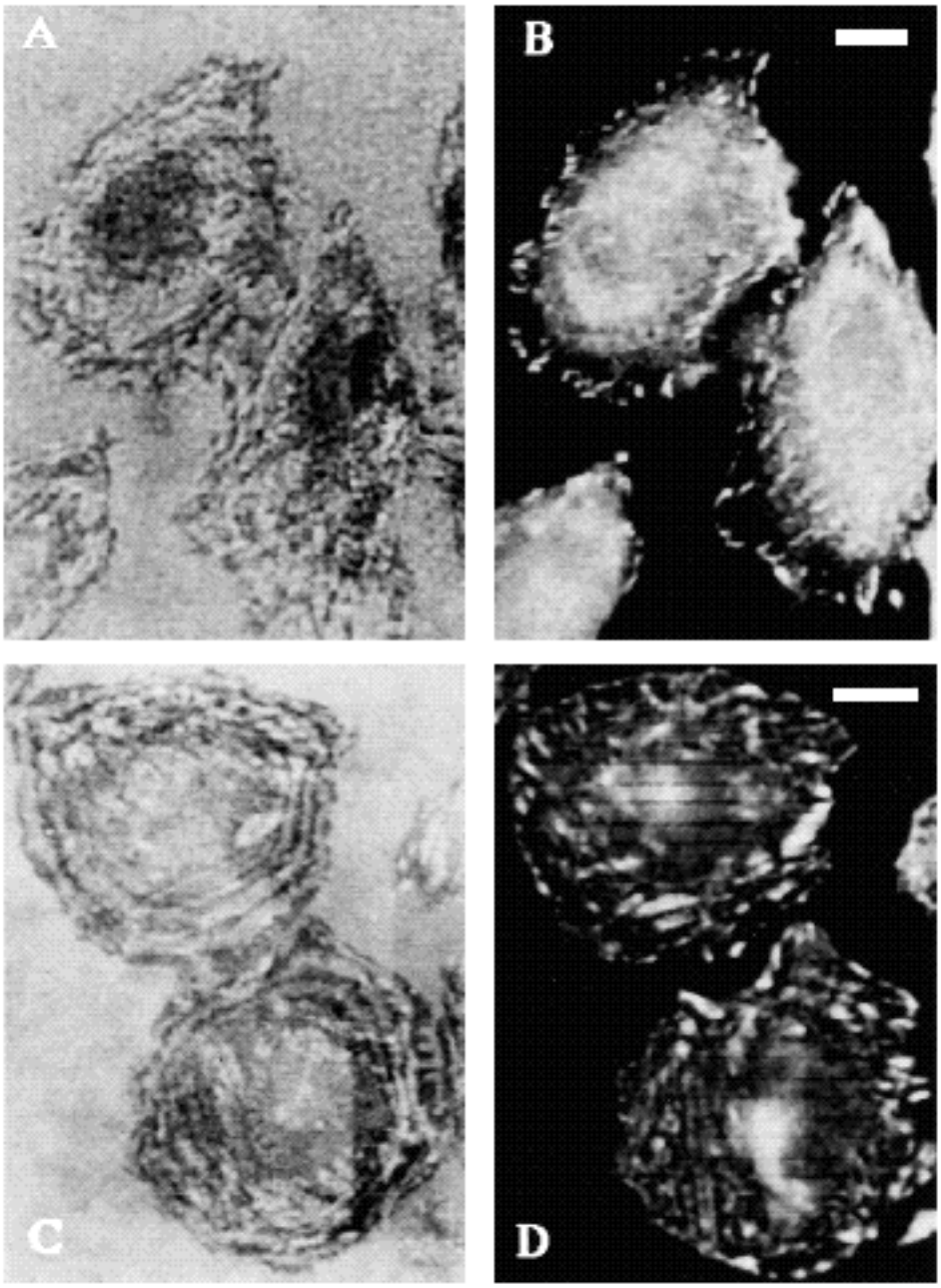

Fig. 5. IRM images of control and CHO cells. The cells were seeded on fibronectin-coated glass coverslips and allowed to attach and spread for 4 h at 37°C. Then the medium was removed and after a wash in PBS, replaced with 3% paraformaldehyde in PBS at 37°C for 10 min. Then the preparation proceeded as described under Materials and Methods for immunostaining with anti-vinculin. Microscopy was performed using a Microphot FxA Nikon microscope equipped for epi-fluorescence and IRM as described under Materials and Methods. (A and B) Control CHO cells. (C and D) Monensin-treated cells. (A and C) IRM images. (B and D) Immunostaining of vinculin. Bars, 10 μm.

edges of the cells remained (Fig. 8). These observations were consistent with the idea that the central focal contacts have a distinct organization as compared to peripheral adhesion plaques.

Further evidence of the heterogeneous nature of cellular adhesive structures was provided by the synergetic effect of PB1 and monensin (Fig. 9). Indeed, the disruption of adhesion plaques by monensin allowed low concentrations of PB1 to detach the cells, presumably by disrupting the remaining focal contacts. On the other hand, these structures seem to have different biological properties: indirect immunofluorescence studies with anti-actin antibodies revealed that stress fibers could be observed in control CHO cells (Fig. 10A). Conversely, with monensin-treated cells, cortical and punctate actin staining was observed but no stress fibers were present (Fig. 10B). Therefore, central contacts were unable on their own to organize the stress fibers. Using classical immunomicroscopy, double immunostaining with anti-actin and anti-vinculin was performed on cells spread out under our standard conditions. Fig. 11 shows that all stress fibers terminated in adhesion plaques specifically stained by anti-vinculin. Microfilaments often linked peripheral and central adhesion plaques. These crosslinks may explain the relative compartmentation of the peripheral and central cell-substratum contacts.

DISCUSSION

The present analysis of the pharmacological inhibition of

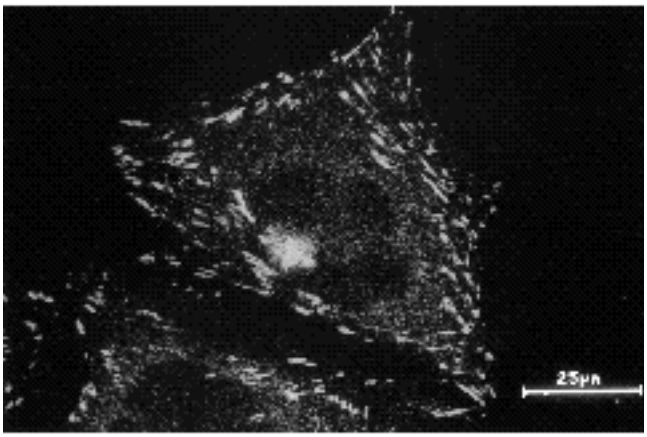

Fig. 6. Views of the adhesive structures in CHO cells after a 24 h incubation period in α-MEM supplemented with 7.5% foetal calf serum. The cells were allowed to attach and spread on a fibronectin-coated coverslip for 24 h at 37°C. Then the medium was removed and after a wash in PBS, replaced with 3% paraformaldehyde in PBS at 37°C. The incubation was carried out for 10 min, and the preparation was subjected to microscopy. Immunostaining was performed with anti-vinculin monoclonal antibodies. Note that no adhesion plaques remain at the center of the cell. Bar, 25 µm.

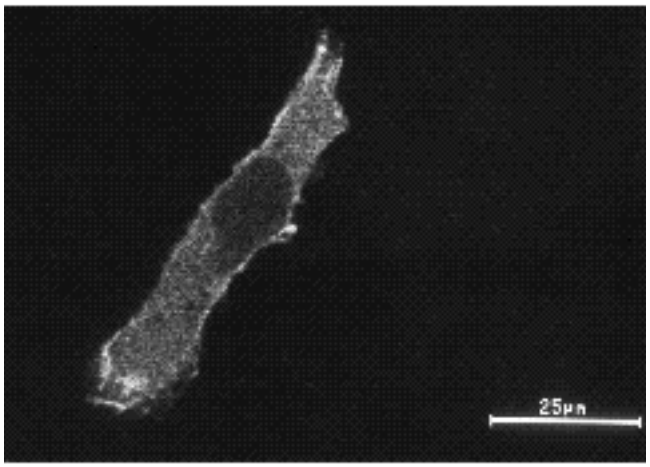

Fig. 8. Cell shape and adhesive structures of spread-out CHO cells treated with anti-FnR PB1. Spread-out CHO cells were incubated at 37°C with PB1 (1 µg/ml) for 4 h. Then the cells were fixed with 3% paraformaldehyde in PBS for 10 min at 37°C. The preparation was subsequently processed as described earlier. Immunofluorescence was performed with the anti-vinculin monoclonal antibody. Bar, 25 µm.

the endocytic cycle of the fibronectin receptors was undertaken to examine the dynamics of the integrins within the cell-substratum contact sites, which can provide transient adhesion or stable anchorage to the extracellular matrix. Evidence of some recycling of the FnRs in CHO cells has been previously reported for CHO cells in suspension (Bretscher, 1989; Sczekan and Juliano, 1990). However, in that case, the integrins were not embedded in the focal contacts and had maximum mobility; yet, only 30% of the FnRs were efficiently internalized, regardless of their ligation state, whereas a much larger fraction seemed to be unavailable for fast endocytosis (Sczekan and Juliano, 1990). Here we report that FnRs may be distributed between distinct sites of cell adhesion to the extracellular matrix with distinct structures. One of these seems to be sensitive to monensin by a mechanism that may involve either receptor recycling or the composition of intracellular ions.

Addition of monensin resulted in a dramatic morphological change in the cells. Since this ionophore is a potent

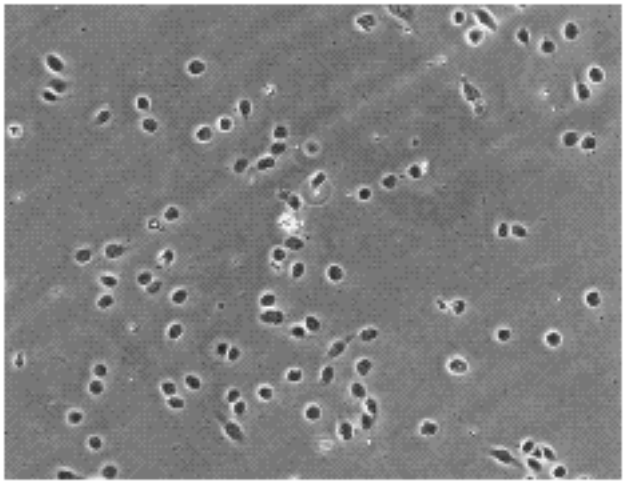

Fig. 7. Sensitivity to monensin of CHO cells spread out on fibronectin for 24 h in foetal calf serum-supplemented medium. The cells were allowed to attach and spread on a fibronectin-coated coverslip for 24 h at 37°C. Then the medium was removed and after a wash in PBS, replaced with fresh α-MEM without calf serum and with monensin (25 µM) for 4 h at 37°C. ×100.

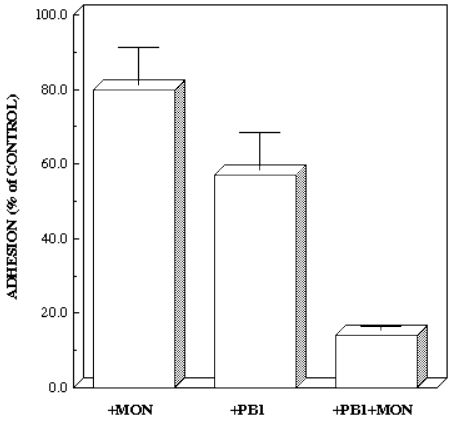

Fig. 9. Synergetic inhibition of cell adhesion by PB1 and monensin. Monensin (25 µM), PB1 (1 µg/ml) or monensin plus PB1 were added to spread-out cells and the incubation was continued for 4 h at 37°C. Then the living cells were washed with PBS and photographed using a phase-contrast objective lens, at a magnification of ×100. For each experimental condition, the number of adhesive cells in a constant area of 0.03 mm^2 was estimated as described under Materials and Methods. These values are compared with those obtained in control experiments (250 cells per area), as a percentage.

Table 2. Thickness of adhesion plaques in CHO cells spread out onto fibronectin-coated dishes

Experimental conditions	Adhesive structures	Staining	Thickness (μm)
Control cells	Peripheral adhesion plaques	Anti-talin	1.1±0.3
		Anti-vinculin	1.3±0.3
		Anti-actin	1.4±0.5
	Central adhesion plaques	Anti-talin	0.8±0.3
		Anti-vinculin	0.7±0.3
		Anti-actin	1.0±0.3
Monensin-treated cells	Adhesion plaques (any localization)	Anti-talin	0.8±0.3
		Anti-vinculin	0.8±0.3
		Anti-actin	1.1±0.5

Indirect immunofluorescence staining was performed as described under Materials and Methods. The errors represent the resolution limit of the microscope. The thickness of the labeling was determined by consecutive optical sections (0.2 μm) and the reconstitution of the image of a transverse cut.

inhibitor of receptor recycling, which most likely acts by raising the pH of the endocytic vesicles (Maxfield, 1982), and/or by lowering the intracellular potasium content (Larkin et al., 1983, 1986), the change in the cell shape

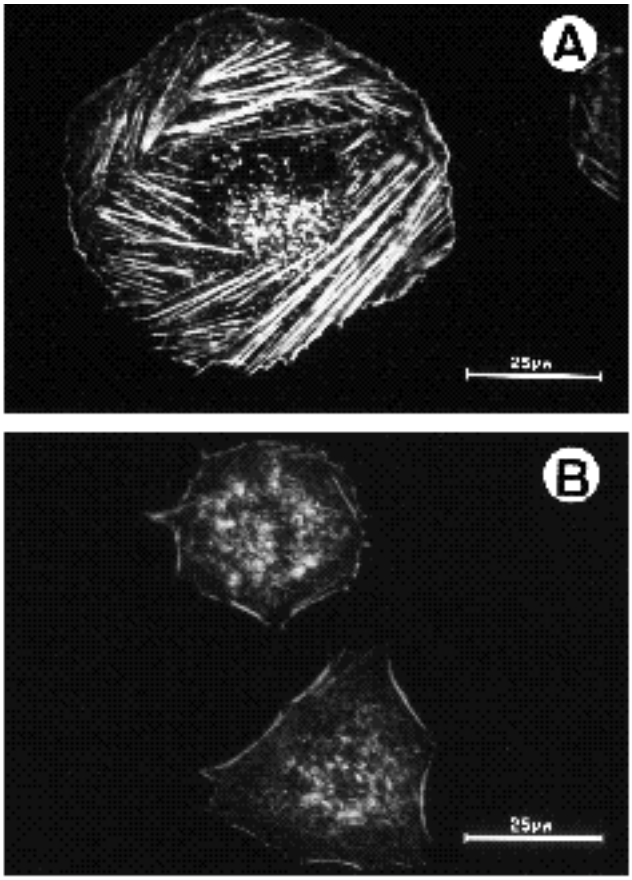

Fig. 10. Adhesion plaques do not support the organization of stress fibers in monensin-treated CHO cells. After 4 h of spreading at 37°C, control and monensin-treated cells were fixed with 3% paraformaldehyde for 10 min at 37°C. Immunostaining with anti-actin monoclonal antibody was performed as described under Materials and Methods. (A) Control cell. (B) Monensin-treated cells. Bars, 10 μm.

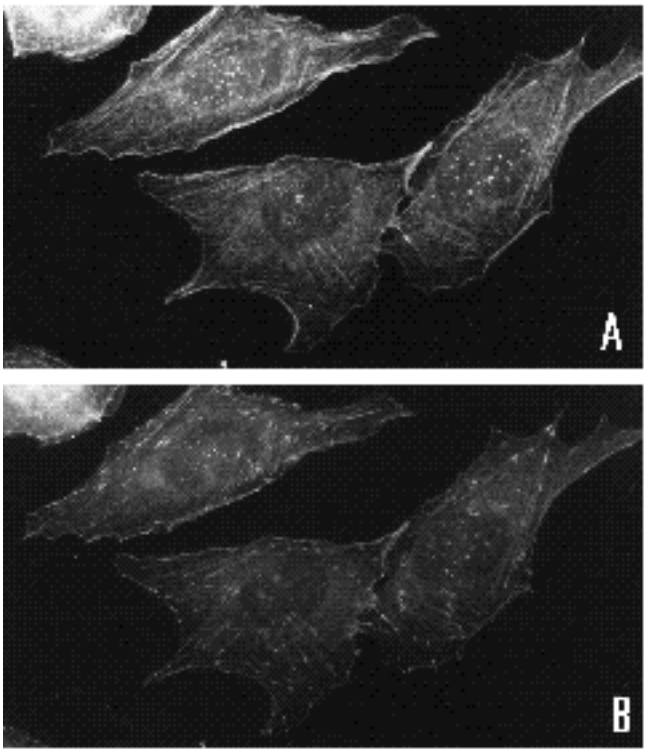

Fig. 11. Double labeling of actin and vinculin on CHO cells after 4 h of spreading at 37°C on fibronectin. The cells were spread on fibronectin-coated coverslips for 4 h at 37°C and processed for immunofluorescence microscopy as described under Materials and Methods. Anti-human FITC$(Fab)_2$ and anti-mouse RITC$(Fab)_2$ were used for actin and vinculin staining, respectively. (A) Actin staining. (B) Vinculin (plus actin) staining.

may be due to inhibition of the endocytic cycle inducing a decrease in the number of the FnRs at the cell surface and the subsequent disorganization of any dynamic cell-substratum contact. This interpretation is supported by a whole line of evidence: (i) monensin did not induce any morphological change in spread-out cells at 4°C, a temperature that blocks endocytosis and vesicular traffic (Table 1). (ii) A similar effect was observed when the carboxylic ionophore monensin was replaced by the permeant amine chloroquine, another inhibitor of cell surface recycling that does not affect the intracellular potassium concentration. (iii) A time-dependent internalization of the fibronectin receptor has been reported, using monensin-treated CHO cells in suspension (Sczekan an Juliano, 1990), and was actually observed with spread-out CHO cells treated with monensin and cycloheximide (Fig. 2).

It has been proposed that internalization of surface proteins occurs when a 'tyrosine internalization signal' is present in the cytoplasmic domain of the receptors. This signal appears to be sufficient to direct transmembrane proteins such as receptors into the endocytic pathway, and to be necessary for the internalization of a variety of cell surface proteins. This generic internalization signal may consist of no more than 8-10 amino acids with a tyrosine residue present in the membrane-distal portion of the sequence. A statistically significant preference for polar or

basic amino acids at specific positions on either side of the tyrosine has been observed together with amino acids that are frequently found in turns and clustered near the tyrosine on the side of the signal nearest the transmembrane domain (Ktistakis et al., 1990). In fact, two tyrosine residues located in putative internalization signals have been identified on the cytosolic stretch of the β_1 chain of chicken and human integrins (Tamkun et al., 1986; Argraves et al., 1987). One of these sequences is homologous to a tyrosine phosphorylation site in the epidermal growth factor receptor. Nevertheless, the β_1 chain seems to be a poor substratum for kinases (Turner et al., 1989) and the replacement of the tyrosine (Tyr788) with a phenylalanine by site-directed mutagenesis resulted in no modification of the behavior of the VLA receptors (Hayashi et al., 1990). However, this sequence may contain several important features of an internalization signal and its role should be reconsidered.

An unexpected outcome of our study was the finding that FnRs are distributed between two types of cell-substratum contacts. These two structures have been distinguished on the basis of their different sensitivity to monensin or chloroquine: the peripheral adhesion plaques are slowly disrupted by monensin or chloroquine, whereas contacts with a more central localization are more resistant to the drugs. Futhermore, these two types of adhesive structures have also distinct structural organizations. Central contacts are thinner (Table 2). Tentative measurements of adhesion plaques were performed earlier by Chen and Singer (1982) using electron microscopy; however, due to the very similar electronic density of the proteinaceous material at the adhesion plaque and in the surrounding cytosol, such a determination was unsucessful. However, Chen and Singer (1982) have given an accurate measurement of the gap between the membrane and the extracellular matrix (0.3-0.5 μm), a value that is significantly smaller than the tickness of the intracellular material located at the focal contacts. Thin adhesive structures have been previously reported when cells are allowed to attach and spread onto RGDS-coated plastic dishes (Streeter and Rees, 1987) or when cells spread onto plastic coated at low density with the synthetic peptide GRGDY (Massia and Hubbell, 1991). Furthermore, the establishment of two types of adhesion plaques has peviously been identified in embryo quail cells (Bershadsky et al., 1985). These authors reported that only one type was associated with actin microfilament bundles and it may represent early adhesive structures. Our present data are very similar even though the distribution of the cell contacts seems quite different in CHO cells compared to quail cells. When CHO cells are allowed to spread for a long time in a medium supplemented with foetal calf serum, a reorganization of the adhesive structures is observed (Fig. 6). Therefore, sequential organization of the cell-matrix contact may occur during the cell cycle. It is noteworthy that after a long time of spreading in serum-supplemented medium the cells are still sensitive to monensin (Fig. 7). Peripheral and central adhesion plaques differ with respect to their biological properties: central contacts cannot alone sustain the organization of the stress fibers (Figs 10 and 11). The sensitivity to monensin of classical (peripheral) adhesion plaques suggests that they are in equilibrium with free integrins, which are subjected to constitutive recycling, and therefore it is likely that they exhibit a high degree of self-renewal. Conversely, the relative resistance to monensin of the central focal contacts indicates that they may be more-static structures, or may be in equilibrium with receptors that are not subjected to the endocytic cycle.

Fibronectin receptor clusters in peripheral or central plaques involved similar fibronectin receptors, since both structures are sensitive to the monoclonal antibody PB1. However, it has been reported recently that alternative variants of the β_1 integrin chain contain distinct cytoplasmic domains (Altruda et al., 1990; Languino and Ruoslahti, 1992). The possibility cannot be excluded that such variants may be involved in different links with the cytoskeleton, or may not be subjected to endocytosis.

In summary, our results suggest that the fibronectin receptors clustered within peripheral adhesion plaques are slowly exchanged with neighboring receptors on the plasma membrane, which are subsequently internalized and recycled from an intracellular pool. On the other hand, central focal contacts exhibit different structures and functions. They are organized early in the adhesion process from receptors that are already present at the cell surface (Fig. 3). These structures may be more static, or may be in equilibrium with FnRs that are not available to the endocytic cycle. Finally, further organization of the adhesion plaques involving other integrins may occur in long-term experiments.

We propose that cells attach and flatten using external receptors clustered in central focal contacts, whereas spreading is achieved by the formation of peripheral adhesion plaques that support stress fibers. The reasons why the same types of integrins are distributed between the distinct structures remain to be elucidated.

We thank Dr J.-L. Duband for helpful discussions and criticisms, and Dr R. L. Juliano for providing us with the monoclonal antibody PB1. This work was supported by the CNRS by the INSERM. (Contrats de recherche externes nos 90 102 and 90 506), and by a grant from the Association pour la Recherche contre le Cancer (ARC).

REFERENCES

Allen, R. D., Allen, N. S. and Travis, J. L. (1981). Video-enhanced contrast, differential interference contrast (AVEC-DIC) microscopy: A new method capable of analyzing microtubule-related motility in the reticulopodial network of *Allogromia paticollaris*. *Cell Motil.* **1**, 291-302.

Altruda, F., Cervella, P., Tarone, G., Botta, C., Balzac, F., Stefanuto, G. and Silengo, L. (1990). A human integrin β_1 subunit with a unique cytoplasmic domain generated by an alternative mRNA processing. *Gene* **95**, 261-266.

Argraves, S. W., Suzuki, S., Arai, H., Thompson, K., Pierschbacher, M. D. and Ruoslahti, E. (1987). Amino acid sequence of the human fibronectin receptor. *J. Cell Biol.* **105**, 1183-1190.

Basu, S. K., Goldstein, J. L., Anderson, R. G. W. and Brown, M. S. (1981). Monensin interrupts the recycling of low density lipoprotein receptors in human fibroblasts. *Cell* **24**, 493-502.

Berg, T., Blomhoff, R., Naess, L., Tolleshaug, H. and Drevon, C. A. (1983). Monensin inhibits receptor-mediated endocytosis of asialoglycoproteins in rat hepatocytes. *Exp. Cell Res.* **148**, 319-330.

Bershadsky, A. D., Tint, I. S., Neyfakh, A. A. Jr and Vasiliev, J. M. (1985). Focal contacts of normal and RSV-transformed quail cells. *Exp. Cell Res.* **158**, 433-444.

Bretscher, M. S. (1989). Endocytosis and recycling of the fibronectin receptor in CHO cells. *EMBO J.* **8**, 1341-1348.

Bretscher, M. S. (1992). Circulating integrins: $\alpha_5\beta_1$, $\alpha_6\beta_4$ and Mac-1, but not $\alpha_3\beta_1$, $\alpha_4\beta_1$ or LFA-1. *EMBO J.* **8,** 405-410.

Brown, P. J. and Juliano, R. L. (1985). Selective inhibition of fibronectin-mediated cell adhesion by monoclonal antibodies to a cell-surface glycoprotein. *Science* **228**, 1448-1450.

Charo, I. F., Nannizzi, I., Smith, J. W. and Cheresh, D. A. (1990). The vitronectin receptor $\alpha_v\beta_3$ binds fibronectin and acts in concert with $\alpha_5\beta_1$ in promoting cellular attachmment and spreading on fibronectin. *J. Cell Biol.* **111**, 2795-2800.

Dedhar, S. (1990). Integrins and tumor invasion. *BioEssays* **12**, 583-590.

Dejana, E., Colella, S., Conforti, G., Abbadini, M., Gaboli, M. and Marchisio, P. C. (1988). Fibronectin and vitronectin regulate the organization of their respective Arg-Gly-Asp adhesion receptors in cultured human endothelial cells. *J. Cell Biol.* **107**, 1215-1223.

Duband, J.-L., Nuckolls, G. H., Ishihara, A., Hasegawa, T., Yamada, K. M., Thierry, J.-P. and Jacobson, K. (1988). Fibronectin receptor exhibits high lateral mobility in embryonic locomoting cells but is immobile in focal contacts and fibrillar streaks in stationary cells. *J. Cell Biol.* **107**, 1385-1396.

Engvall, E. and Ruoslahti, E. (1977). Binding of soluble form of fibroblast surface protein, fibronectin, to collagen. *Int. J. Cancer* **20**, 1-5.

Gonalez-Noriega, A., Grupp, J. H., Talkad, V. and Sly, W. S. (1980). Chloroquine inhibits lysosomal enzyme secretion by impairing receptor recycling. *J. Cell Biol.* **82**, 839-852.

Granger, B. L. and Lazarides, E. (1979). Desmin and vimentin coexist at the periphery of the myofibril Z disc. *Cell* **18**, 1053-1063.

Harford, J., Bridges, K., Ashwell, G. and Klausner, R. D. (1983a). Intracellular dissociation of receptor bound asialoglycoproteins in cultured hepatocytes. *J. Biol. Chem.* **258**, 3191-3197.

Harford, J., Wolkoff, W., Ashwell, G. and Klausner, R. D. (1983b). Monensin inhibits intracellular dissociation of asialoglycoproteins from their receptors. *J. Cell Biol.* **96**, 1824-1828.

Hayashi, Y., Haimovich, B., Reszka, A., Boettiger, D. and Horwitz, A. (1990). Expression and function of chicken integrin b1 subunit and its cytoplasmic domain mutants in mouse NIH 3T3 cells. *J. Cell Biol.* **110**, 175-184.

Hemler, M. E. (1990). VLA proteins in the integrin family: structures, functions, and their role on leucocytes. *Annu. Rev. Immunol.* **8**, 365-400.

Hynes, R. O. (1992). Integrins: Versatility, modulation and signaling in cell adhesion. *Cell* **69**, 11-25.

Ktistakis, N. T., D'Nette, T. and Roth, M. G. (1990). Characteristics of the tyrosine recognition signal for internalization of transmembrane surface glycoproteins. *J. Cell Biol.* **111**, 1393-1407.

Languino, L. R. and Ruoslahti, E. (1992). An alternative form of the integrin β_1 subunit with a variant cytoplasmic domain. *J. Biol. Chem.*. **267**, 7116-7120.

Larkin, J. M., Brown, M. S., Goldstein, J. L. and Anderson, R. G. W. (1983). Depletion of intracellular potassium arrests coated pits formation and receptor mediated endocytosis in fibroblasts. *Cell* **33**, 273-285.

Larkin, J. M., Donzell, W. C. and Anderson, R. G. W. (1986). Potassium dependent assembly of coated pits : new coated pits form as planar clathrin lattices. *J. Cell Biol.* **103**, 2619-2627.

Massia, S. P. and Hubbell, J. A. (1991). An RGD spacing of 440nm is sufficient for integrin $\alpha_v\beta_3$-mediated fibroblast spreading and 140 nm for focal contact and stress fiber formation. *J. Cell Biol.* **114**, 1089-1100.

Maxfield, F. R. (1982). Weak bases and ionophores rapidly and reversibly raise the pH of endocytic vesicles in cultured mouse fibroblasts. *J. Cell Biol.* **95**, 676-681.

Ruoslahti, E. (1991). Integrins. *J. Clin. Invest.* **87**, 1-5.

Russ, J. C. (1990). Computer-assisted microscopy. In *The Measurement and Analysis of Images*. Plenum Press, New York and London.

Sczekan, M. M. and Juliano, R. L. (1990). Internalization of the fibronectin receptor is a constitutive process. *J. Cell. Physiol.* **142**, 574-580.

Streeter, H. B. and Rees, D. A. (1987). Fibroblast adhesion to RGDS shows novel features composed with fibronectin. *J. Cell Biol.* **105**, 507-515.

Tamkun, J. W., Desimone, D. W., Fonda, D., Patel, R. S., Buck, C., Horwitz, A. F. and Hynes, R. O. (1986). Structure of integrin, a glycoprotein involved in the transmembrane linkage between fibronectin and actin. *Cell* **46**, 271-282.

Tranqui, L., Soyez, S. and Block, M. R. (1992). An in vitro model giving access to adhesion plaques. *In Vitro Cell. Dev. Biol.* **28A**, 17-23.

Turner, C. E. and Burridge, K. (1988). Detection of metavinculin in human platelets using a modified talin overlay assay. *Eur. J. Cell. Biol.* **49**, 202-206.

Turner, C. E. and Burridge, K. (1991). Transmembrane molecular assemblies in cell-extracellular matrix interactions. *Curr. Opin. Cell. Biol.* **3**, 849-853.

Turner, C. E., Pavalko, F. M. and Burridge, K. (1989). The role of phosphorylation and limited proteolytic cleavage of talin and vinculin in the disruption of focal adhesion integrity. *J. Biol. Chem.* **264**, 11938-11944.

Van Leuven, F., Cassiman, J. J. and Van Den Berghe, H. (1980), Primary amines inhibit recycling of α_2M receptors in fibroblasts. *Cell* **20**, 37-43.

(Received 27 October 1992 - Accepted, in revised form, 12 May 1993)